DNA synthesis from diphosphate substrates by DNA polymerases

Cassandra R. Burke[a,1] and Andrej Lupták[a,b,c,2]

[a]Department of Chemistry, University of California, Irvine, CA 92697; [b]Department of Pharmaceutical Sciences, University of California, Irvine, CA 92697; and [c]Department of Molecular Biology and Biochemistry, University of California, Irvine, CA 92697

Edited by Jack W. Szostak, Massachusetts General Hospital, Boston, MA, and approved December 22, 2017 (received for review July 8, 2017)

The activity of DNA polymerase underlies numerous biotechnologies, cell division, and therapeutics, yet the enzyme remains incompletely understood. We demonstrate that both thermostable and mesophilic DNA polymerases readily utilize deoxyribonucleoside diphosphates (dNDPs) for DNA synthesis and inorganic phosphate for the reverse reaction, that is, phosphorolysis of DNA. For Taq DNA polymerase, the K_Ms of the dNDP and phosphate substrates are ∼20 and 200 times higher than for dNTP and pyrophosphate, respectively. DNA synthesis from dNDPs is about 17 times slower than from dNTPs, and DNA phosphorolysis about 200 times less efficient than pyrophosphorolysis. Such parameters allow DNA replication without requiring coupled metabolism to sequester the phosphate products, which consequently do not pose a threat to genome stability. This mechanism contrasts with DNA synthesis from dNTPs, which yield high-energy pyrophosphates that have to be hydrolyzed to phosphates to prevent the reverse reaction. Because the last common ancestor was likely a thermophile, dNDPs are plausible substrates for genome replication on early Earth and may represent metabolic intermediates later replaced by the higher-energy triphosphates.

DNA replication | transition state | activation energy | energy charge | phosphorolysis

All living organisms are thought to utilize deoxyribonucleoside triphosphates (dNTPs) as substrates for genome replication by DNA polymerases, which are responsible for both replication and repair of cellular DNA. These enzymes catalyze the transfer of the α-phosphate of the incoming nucleotide from its β-phosphate to the 3′ hydroxyl of the primer. The γ-phosphate of the dNTP does not play a direct role in catalysis, but aids in driving the polymerization as part of the pyrophosphate (PP_i) leaving group, making the triphosphate a higher energy substrate than diphosphate by ∼13 kJ/mol (1, 2). The pyrophosphate product of the reaction is a high-energy metabolic intermediate that is further hydrolyzed by pyrophosphatases into two molecules of phosphate. This coupled breakdown of pyrophosphate is necessary to drive the DNA (and RNA) synthesis forward because the activation energy of the reverse reaction—pyrophosphorolysis of DNA (3)—is thought to be only ∼17 kJ/mol (∼4 kcal/mol) higher than for the forward reaction (4), and pyrophosphates are produced at high rates by both transcription and replication. In thermophiles, this system may not be necessary because DNA polymerases may be able to effectively trade the ground-state energy of the activated substrates for kinetic enhancement due to elevated temperature, and the reverse reaction may be inefficient due to lower phosphate affinity. Here we show that several thermostable DNA polymerases, including a bacterial replicative polymerase, and the mesophilic *Bacillus subtilis* (*Bsu*) DNA polymerase I, can substitute the canonical triphosphate substrates with their diphosphate analogs in DNA replication. Furthermore, we measured the kinetic parameters and activation energies for the forward and reverse reactions and provide a mechanistic framework for understanding replication of DNA from dNDP substrates.

Results and Discussion

We began by testing Taq (from *Thermus aquaticus*), high-fidelity Vent (exo−, from *Thermococcus litoralis*), *Pfu* (exo+, from *Pyrococcus furiosus*), Deep Vent (exo+, from *Pyrococcus* sp. GB–D), and Q5 (exo+) DNA polymerases in traditional polymerase chain reactions (PCR) with a deoxyribonucleoside monophosphate (dGMP), dNDPs, and dNTPs as substrates (Fig. 1 *A* and *B*). Substitution of any of the dNTPs for dNDPs supported robust DNA synthesis, and further experiments with two, three, or all four dNDPs instead of dNTPs supported PCR. To ensure that the products did not result from contaminating dNTPs and that the reactions were not enhanced by stabilizers present in commercial buffers or enzyme stocks, we tested DNA synthesis from purified dNDPs using homemade buffers and enzymes. We also included bacterial replicative enzymes, such as the bacterial replicative DNA polymerases from the thermophilic *Bacillus stearothermophilus* (*Bst*) and the mesophilic *Bacillus subtilis* (*Bsu*, large fragment). These, together with archaeal polymerases from *Thermococcus kodakensis* (KOD), *Thermococcus* sp. 9°N (9°N), and *Thermococcus gorganarius* (*Tgo*), showed robust primer extensions using just 100 μM of purified dNDPs at 60 °C (except *Bsu*, which was tested at 37 °C in all instances) (Fig. 1*C*). The primer-extension reactions were efficient for all of these enzymes, particularly for Deep Vent, KOD, and 9°N. Pausing was observed before incorporation of dA and dC into the nascent oligonucleotide (Fig. 1 *C* and *D*), suggesting that the K_Ms for the dADP and dCDP are high enough to slow down the primer extension at a 100-μM substrate concentration.

Significance

All extant cellular organisms are thought to replicate their genomes using triphosphorylated substrates (dNTPs). Because only the α-phosphate is retained in the DNA backbone, both dNTPs and diphosphates (dNDPs) can in principle drive DNA synthesis. The activation barrier for the transphosphorylation is expected to be higher for dNDPs than for dNTPs, rendering the dNDP reactions slower; however, at elevated temperatures this penalty may be less prohibitive. We demonstrate DNA synthesis from dNDPs for a number of DNA polymerases, including bacterial and archaeal replicative and repair enzymes. Activation energy analysis of the forward (DNA synthesis) and reverse (phosphorolysis of DNA) reactions catalyzed by the Taq DNA polymerase shows that DNA synthesis is strongly favored, allowing surprisingly robust replication from low-energy substrates.

Author contributions: C.R.B. and A.L. designed research, performed research, analyzed data, and wrote the paper.

The authors declare no conflict of interest.

This article is a PNAS Direct Submission.

[1]Present address: Molecular Engineering and Sciences Institute, Department of Chemical Engineering, University of Washington, Seattle, WA 98195.

[2]To whom correspondence should be addressed. Email: aluptak@uci.edu.

This article contains supporting information online at www.pnas.org/lookup/suppl/doi:10.1073/pnas.1712193115/-/DCSupplemental.

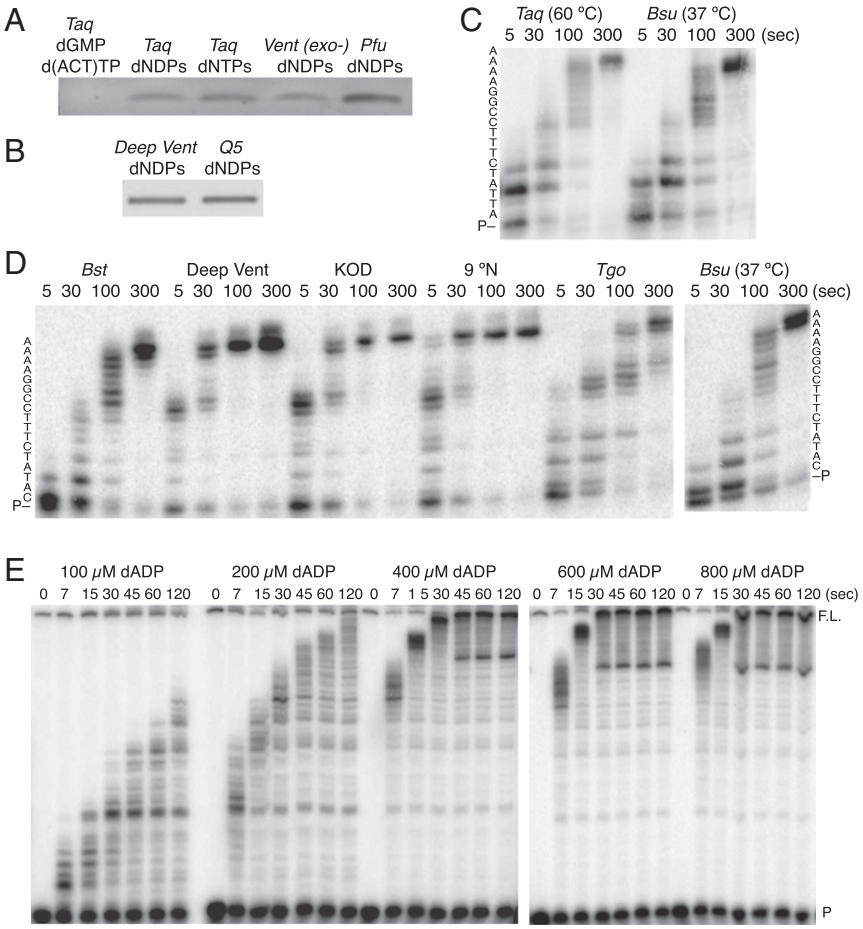

Fig. 1. Deoxynucleoside diphosphate utilization by DNA polymerases. (*A*) A standard PCR with a monophosphate substrate is inhibited, whereas the presence of all four di- or triphosphate nucleotides supports DNA amplification. Thermophilic polymerases Taq, Vent (exo–), and *Pfu*, as well as *B*, Deep Vent, and Q5 DNA polymerases, also utilize the diphosphorylated substrates. (*C* and *D*) Primer-extension reactions on short templates sampled at indicated time points. All reactions were performed with 100 μM dNDPs at 60 °C, except the *Bsu* reactions, which were performed at 37 °C. Extended sequences are shown alongside of gels and were distinct in *C* and *D*. Primer band is indicated with "–P." Pausing appears mainly before incorporation of dA and dC and is variable among the polymerases. (*E*) Primer-extension assay with dCTP, dGTP, dTTP, and increasing concentrations of dADP. The reactions were quenched at varying time points between 7 and 120 s. The primer (P) and full-length (F.L., 706 nt) products were resolved on a denaturing polyacrylamide gel. Pausing was observed only for the case of dADP incorporation. Analysis of the rate of full-length DNA production yields a half-maximal rate at ~420 μM dADP (Fig. S2*B*).

To gain a mechanistic insight into the reaction, we first studied its efficiency using the Taq enzyme. Varying the extension temperature from 50 °C to 72 °C resulted in no observable difference in the quantity of full-length product. To simplify the kinetic analyses, all PCR reactions were performed using a two-step temperature cycling protocol, in which the primer was annealed and extended in the first step at 72 °C and the duplex melted at 95 °C in the second step (Fig. S1*A*). To compare the rates of dNDP utilization to the canonical dNTPs, the extension time was varied from 15 to 120 s. For a 15-s extension time, the dNTP reaction produced approximately four times the product compared with the 2-min extension time reaction that contained the dNDPs (Fig. S1*B*). These data suggested that the rate of incorporation for the diphosphates is slower than that of the traditional triphosphates, as would be expected considering the lower ground-state energy of the dNDPs. We next asked whether a single or all four dNDPs are responsible for the slower incorporation rate. Quantitative PCR (qPCR) was used for an accurate measurement of product formation. Each diphosphate was interrogated independently by combining it with 0.2 mM of the other three dNTPs to amplify a long DNA template. These reactions were normalized to a control reaction, which contained 0.2 mM of all four dNTPs (Fig. S1*C*). A value of 1 indicates that a diphosphate is incorporated as efficiently as its triphosphate analog. These results suggest that dADP is incorporated least efficiently (1 mM dADP yielded ~60% of 0.2 mM dATP), followed by deoxythymidine diphosphate (dTDP) and deoxycytidine diphosphate (dCDP). On the other hand, only a twofold increase in the concentration of dGDP is necessary to reach the same PCR efficiency as the dGTP control reaction.

To analyze the DNA polymerization directly, we performed a primer extension reaction of a ^{32}P-labeled primer and a long (706 nt) template. The diphosphate concentration was varied from 0.1 to 1.0 mM and combined with 0.2 mM of the other three dNTPs, similar to the qPCR reactions described above. As expected, increasing concentrations of dADP decreased the amount of time necessary to produce full-length product (Fig. 1*E*). Pausing along the length of the template DNA was observed solely in the case of dADP, suggesting that the polymerase stalls during the incorporation of dADP substrates (Fig. 1*E*). On the other hand, the lack of pausing in the dTDP reaction suggested that dTDP was more efficiently utilized than dADP (Fig. S2*A*), as suggested by the qPCR analysis (Fig. S1*A*). Analysis of product formation suggested that dADP concentration required to reach half-maximum rate is ~420 μM (Fig. S2*B*), more than an order of magnitude above K_M for dNTPs measured previously (16 and 24 μM) (5, 6). Near saturating concentration of dADP, the full-length DNA is synthesized in about 30 s and, given that the 706-nt sequence contains 182

adenosines, the average speed of utilization of dADP is at least ~6 s^{-1}. This is about an order of magnitude slower than the average speed of utilization of dNTPs by the Taq polymerase (k_{cat} = 47 s^{-1}) and is within 1.5-fold of the k_{cat} of *Pfu* (7).

To further compare the kinetics of DNA synthesis on long templates from dNDPs and dNTPs, we used a singe-stranded DNA (ssDNA) M13mp18 plasmid template of 7,249 nt (8). *Bsu* (at 37 °C), *Bst*, and Taq (at 60 °C) polymerases showed robust DNA synthesis from dNDPs (Fig. S2*C*). We measured the rate of DNA synthesis using the fluorescence of the SYTO9 intercalator, observed by a real-time thermal cycler at varying dNDP and dNTP concentrations (Fig. S2*D*) (9). A plot of these rates versus nucleotide concentration revealed an apparent K_M of ~0.4 mM for dNDPs and a maximum rate of synthesis that is about 17 times lower for dNDPs than for dNTPs (Fig. S2*E*). These results show, in a direct comparison under identical conditions, that the rate of DNA synthesis from dNDPs is a little over an order of magnitude lower than from dNTPs and that V_{max}/K_M is thus about 400 times lower for dNDPs than for dNTPs.

A polymerization reaction with canonical triphosphate substrates increases the length of the nascent DNA strand by one nucleotide, releasing a PP_i (3). During the reverse reaction, pyrophosphorolysis, the primer is shortened by one nucleotide and a dNTP is released. Analogously, when dNDPs are used as substrates, polymerases release phosphates, and the reverse reaction is phosphorolysis of DNA (Fig. 2*A*). To confirm that the polymerases utilize dNDPs directly and do not use a hitherto unknown enzymatic activity (or copurified nucleotide diphosphate kinase) that converts two dNDPs into a dNTP and a dNMP, we used purified dNDPs and analyzed the products of a primer-extension reaction. We measured the production of phosphate using a fluorescent sensor, which is derived from the bacterial phosphate-binding protein and exhibits a high specificity for phosphate (10). We found that, in the presence of purified dNDPs and Taq DNA polymerase, phosphate builds up (Fig. 2*B*), but in experiments lacking the polymerase, it does not. In control experiments with dNTPs, phosphate production was observed, but its rate was slower and independent of the enzyme, suggesting that the detected phosphate resulted from dNTP degradation to dNDP and phosphate and was not related to DNA synthesis. These results confirmed that Taq directly utilizes dNDPs as substrates, releasing phosphate as the by-product of the DNA synthesis. When we measured the amount of phosphate produced in primer extensions on the 7,249-nt M13 ssDNA described above, we found that ~1–11 μM phosphate was produced using a 1.6-nM template over background phosphate production from dNDP degradation (Fig. S3*A*). This phosphate concentration corresponds to ~2–6,000 molecules per DNA, or about 0.1–0.9 of the template copied using dNDPs. The wide range results from a relatively large phosphate background in the starting material and the background reaction subtracted from the signal in the primer-extension reaction.

To verify that the reactions do not produce dNTPs from dNDPs, we incubated the Taq polymerase with 250 μM of dCDP and dTDP and resolved the reactions by ion-exchange chromatography (Fig. S3*B*). This analysis did not reveal any new molecular species corresponding to mono- or triphosphorylated nucleotides in the enzyme-containing reaction, compared with the enzyme-free reaction, indicating a lack of phosphoryl transferase activity in the enzyme preparation and further supporting direct utilization of dNDPs in DNA synthesis.

As described above, reactions with dNDP substrates release an inorganic phosphate (P_i), and the reverse reaction is thus phosphorolysis of DNA (Fig. 2*A*). To test the efficiency of this reverse reaction, we investigated the phosphorolysis of a 5′ ^{32}P-labeled primer annealed to a template strand by incubating it with the enzyme and 10 mM P_i. Fig. 2*C* shows the removal of the terminal 3′ nucleotide from the primer strand by Taq DNA polymerase in the presence of P_i and PP_i, demonstrating that Taq DNA polymerase can undergo the reverse reaction of DNA polymerization from both dNTPs and dNDPs. Analysis of the thermophilic *Bst*, Deep Vent, KOD (Fig. S4*A*), 9°N, *Tgo*, and the mesophilic *Bsu* polymerases also showed phosphorolysis of DNA (Fig. S4*B*), albeit to a lesser extent. A control reaction with the Klenow fragment of the *Escherichia coli* DNA polymerase I, which does not accept dNDPs as substrates, was also examined (Fig. S4*C*) and showed that the presence of PP_i, but not P_i, results in the shortening of the primer.

To further analyze the reverse reaction, we prepared dsDNA labeled internally with ^{32}P-phosphate by performing a primer extension reaction using α–^{32}P-dATP, followed by PAGE purification. We analyzed the products of the reverse reaction using

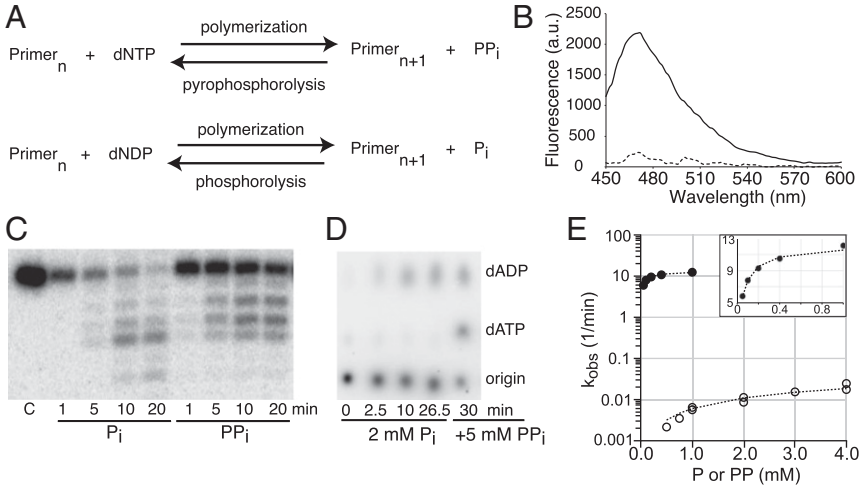

Fig. 2. DNA phosphorolysis by Taq DNA polymerase. (*A*) Scheme of forward and reverse reactions with dNTPs/dNDPs and pyrophosphate/phosphate as substrates, respectively. (*B*) Phosphate-specific fluorescent sensor revealed phosphate in a Taq-catalyzed primer-extension reaction with purified dNDPs (solid line). No fluorescence was observed when the enzyme was omitted (dashed line). (*C*) Inorganic phosphate (P_i)- and pyrophosphate (PP_i)-dependent reverse reactions over 20 min show digestion of the 5′ labeled primer. (*D*) Anion-exchange TLC analysis of products released during the reverse reaction. Incubation of Taq polymerase in the presence of phosphate (P_i) and a ^{32}P-labeled primer yields ^{32}P-dADP, and addition of 5 mM pyrophosphate to the reaction also yields ^{32}P-dATP, providing further evidence that Taq DNA polymerase can utilize both di- and triphosphate substrates for polymerization. (*E*) DNA degradation with phosphate (○) and pyrophosphate (●), showing large differences in K_M (~10 and 0.054 ± 0.005 mM) and V_{max} (0.0010 ± 0.0005 and 0.205 ± 0.005 s^{-1}, respectively). The pyrophosphate data were fit directly (linear-scale *Inset*), whereas the parameters for phosphate were extracted from a double-reciprocal plot of the data.

anion exchange (polyethyleneimine) TLC. As expected, incubation of the internally labeled DNA with Taq polymerase and pyrophosphate yielded products that comigrated with dATP. Reactions in the presence of phosphate produced faster-migrating species, corresponding to dADP, and reactions without phosphate or pyrophosphate did not produce any migrating species, indicating that in the presence of Taq polymerase alone the DNA remained intact (Fig. 2*D*) and confirming that the reverse reaction is phosphorolysis of DNA.

Finally, analysis of the substrate-dependent kinetics of the reverse reaction revealed a K_M of ∼10 ± 5 mM (n = 9) and 57 ± 5 μM (n = 5) for phosphate and pyrophosphate, respectively, although low solubility of magnesium phosphate above 10 mM precluded us from obtaining precise measurements (Fig. 2*E*). Crystal structures of DNA polymerases with pyrophosphate or phosphonoformic acid in the active sites show a Coulombic interaction with the protein (11–13). The 200-fold ratio between the K_Ms of the two substrates corresponds to ∼15 kJ/mol (3.6 kcal/mol) at 72 °C, a binding energy approximately equal to an ionic interaction between the additional phosphate and a compensating cation on the protein and supporting a model in which the phosphate/pyrophosphate is recognized chiefly through a charge–charge interaction. Estimates of the maximum rates of the reverse reaction followed a similar trend: at these conditions, V_{max} was 0.0010 ± 0.0005 s^{-1} and 0.205 ± 0.005 s^{-1} for phosphate and pyrophosphate, respectively, revealing again an about 200-fold ratio between the two activities. Taken together, below saturating concentrations of the two substrates, the phosphate reaction is about 4×10^4 times less efficient, suggesting that phosphorolysis of DNA does not pose a significant threat to the stability of the genome.

To gain further insight into DNA synthesis from the low-energy substrates (dNDPs and P_i), we measured the activation energies using the Arrhenius analysis of the forward and reverse reactions. Because single-molecule measurements of conformational changes associated with recognition and incorporation of the correct dNTPs revealed faster protein motion than the observed reaction kinetics (14), the rate-limiting step of the forward reaction in the Taq polymerase is likely related to the chemistry step or a pre-catalytic active-site rearrangement that depends on the interaction with the substrate phosphates. We observed that the V_{max} of both forward and reverse reactions is lower for dNDP and phosphate than for dNTP and pyrophosphate, suggesting that the rate-limiting step is sensitive to the phosphorylation state of the substrates. However, both the pre-catalytic rearrangement (such as alignment of active-site residues and binding of a catalytic Mg^{2+} ion) and the chemistry step can be affected by the substrate phosphorylation; therefore, either step can be rate-limiting in the presence of dNDPs, assuming that they do not introduce a new slow conformational step in the mechanism. In Pol β, these two steps have previously been proposed to have similar rate constants (15), and the calculated activation energies for the forward and reverse reactions utilizing the high-energy substrates (dNTPs and pyrophosphate) differ by as little as 15 kJ/mol (4). In the case of the thermophilic Taq and Klentaq1 enzymes, the activation energy of the forward reaction varies widely, ranging from 90 to 125 kJ/mol, depending on the experimental conditions and likely the identity of the reacting nucleotides (8, 16), whereas the activation energy of pyrophosphorolysis has not been, to our knowledge, experimentally determined.

We analyzed single-nucleotide incorporation rates of 50 μM of dCDP, dADP, and dTDP, stacking on dA, dC, and dA, respectively, during the primer-extension reaction. Arrhenius analysis showed a linear dependence of $\ln(k_{obs})$ on 1/T for experiments below 60 °C, revealing activation energies of 85 ± 14, 108 ± 11, and 112 ± 15 kJ/mol for the three nucleotides (Fig. 3 *A* and *B*; n = 6 for each nucleotide). Arrhenius analysis of the reverse reaction with 0.4 mM phosphate, yielding a molecule of dADP, revealed a large activation energy of 138 ± 10 kJ/mol (n = 5), in line with the observed slow rate of DNA phosphorolysis by Taq (Fig. 3 *A* and *B*), and representing a significant increase over the calculated activation energy of pyrophosphorolysis (92 kJ/mol in Pol β) (4). The activation energy of forward and reverse reactions for dADP thus differs by ∼30 kJ/mol, providing a strong bias for DNA synthesis. This bias for the forward reaction results in a lower requirement for sequestration of the phosphate product by a downstream metabolic pathway, in contrast to the dNTP-based DNA synthesis and pyrophosphate hydrolysis by inorganic pyrophosphatases. Furthermore, if the pre-catalytic conformational changes in the Taq polymerase are not affected by the low-energy substrates and the chemistry step is rate-limiting, utilization of dNDPs and phosphates may yield new experimental insight into the enzymatic catalysis of DNA synthesis.

Our study demonstrates that Taq, and several other enzymes from both A and B families of DNA polymerases, including replicative enzymes of both thermophilic and mesophilic bacteria, can substitute the canonical triphosphate substrates with the diphosphate analogs. Early evidence into the expendability of the γ-phosphate in the nucleotide substrate arose from studies of HIV-1 reverse transcriptase and bacteriophage RB69 DNA polymerase gp43. HIV-1 RT variants that abolish the electrostatic interaction between the γ-phosphate of the incoming dNTP and the polymerase resulted in the retention of activity, although at a much slower rate (17–19), and bacteriophage RB69 DNA polymerase gp43 exhibited similar activity (20). Both of these viral enzymes accept dNDPs as substrates, but with K_M (or K_D) that are 500 and 17 times higher, and rate constants that are 100 and 400 times lower than for dNTPs by the HIV-1 RT and RB69 gp43, respectively (20, 21). Our study demonstrates that cellular replicative polymerases possess this activity, describes the substrate affinities and activation energies for both forward and reverse reactions, and implies that DNA synthesis from dNDPs is reasonably efficient, particularly for the thermostable enzymes.

Our results suggest that DNA replication can be accomplished using dNDPs as substrates. In thermophiles, genome replication may be less sensitive to the energy charge of the cell than in mesophiles because thermostable polymerases can accept the diphosphorylated as well as the triphosphorylated substrates. DNA replication is thus less affected by the intracellular ATP/ADP ratio, and the relatively high efficiency with which DNA is synthesized at elevated temperatures suggests that thermophiles may be able to dispense with the triphosphorylated substrates entirely. Furthermore, paleobiological evidence suggests that the last common ancestor of our biosphere was a thermophile (22–24), and our study implies that the disphosphorylated substrates might have been sufficient for genome replication of early organisms, alleviating the need for the metabolism of high-energy triphosphorylated metabolic intermediates. In such a case, the diphosphates could be considered intermediates in the evolution of the high-energy metabolites and may include ancestral building blocks of early genomes, such as ribonucleotides or simpler nucleic acids.

DNA polymerase plays prominent roles in numerous biotechnologies. The use of diphosphate substrates reported here has the potential to make practical the incorporation of expensive analogs, such as isotopically labeled or chemically modified nucleotides, eliminating the need for challenging triphosphate syntheses. This feature of DNA polymerases may also provide a method for detecting nucleotides used in high-throughput DNA sequencing. Two common methods detect the PP_i leaving group associated with primer extension, either through a secondary chemiluminescent assay or by monitoring a change in local pH (25, 26). The use of a dNDP substrate yields P_i, thus offering an additional opportunity to distinguish between incorporated nucleotides. This expanded appreciation for the capabilities of DNA polymerase also suggests that examination of other triphosphate-dependent enzymes could reveal tolerance for lower-energy, easier-to-access, diphosphate substrates as evolutionary intermediates.

Materials and Methods

Materials. Taq DNA polymerase, Phusion High-Fidelity DNA polymerase, DeepVent DNA polymerase, Vent DNA polymerase, Q5 DNA High-Fidelity polymerase, *Bst* polymerase, *Bsu* DNA polymerase (large fragment), and

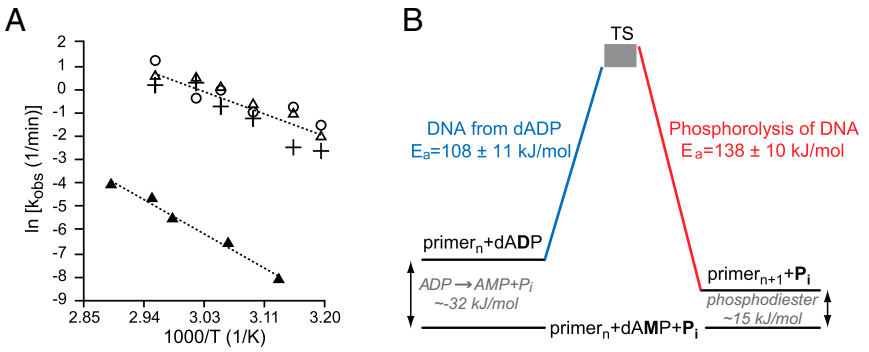

Fig. 3. Kinetic parameters of the forward and reverse reactions with Taq DNA polymerase. (*A*) Arrhenius analysis of the phosphorolysis (to produce dADP; ▲) and the forward reaction with dNDPs, yielding E_a of 138 ± 10 and 90 ± 10 kJ/mol, respectively (108 ± 11, 85 ± 14, and 112 ± 15 kJ/mol for dADP, △; dCDP, ○; and dTDP, +, respectively). (*B*) Reaction coordinate for the forward and reverse reactions, shown relative to the energy of an unextended primer, dAMP (assumed to be the same as the AMP value), and phosphate (P_i). Adding the measured activation energies to the energy of hydrolysis of ADP and a phosphodiester reveals the transition state (TS) to be at about the same level for the forward and reverse reactions (within experimental error, indicated by the gray box). The large difference in activation energies and K_Ms for dNDPs and phosphate, together with the exergonic nature of the overall reaction, explain the efficiency of DNA synthesis from dNDPs, particularly by the thermophilic DNA polymerases, and the apparent stability of DNA with respect to phosphorolysis under either low- or high-energy charge of the cell.

ThermoPol Reaction Buffer [1×: 20 mM Tris·HCl, 10 mM $(NH_4)_2SO_4$, 10 mM KCl, 2 mM $MgSO_4$, 0.1% Triton–X–100, pH 8.8 at 25 °C] were purchased from New England Biolabs. *Pfu*, DeepVent (used in primer extension reaction presented in Fig. 1*D*), KOD, and 9°N DNA polymerases were expressed and purified in-house (27). Deoxynucleotide triphosphates and diphosphates were purchased from Sigma-Aldrich. Deoxynucleotide diphosphates were used as received unless otherwise stated. All DNA oligonucleotides were purchased from Integrated DNA Technologies. All oligonucleotides were used as synthesized unless otherwise stated. Potassium phosphate and potassium pyrophosphate salts were purchased from Sigma-Aldrich. Oregon Green 488 and SybrGreen were from Invitrogen.

Methods.

Monophosphate assay. Taq DNA polymerase (2.5 U) was combined with 0.5 mM each of dATP, dCTP, and dTDP; 0.5 mM of dGMP; 1 μM each of Primer4F and Primer4R; and 0.1 nM of 130-bp template in 1× Taq Buffer. The reaction proceeded at 95 °C for 30 s, 50 °C for 30 s, and 72 °C for 1 min for 16 cycles. Samples were analyzed on a 2% agarose gel and stained with ethidium bromide.

Polymerase screening assay. 2.5 units of each polymerase (Taq, DeepVent, Q5 High-Fidelity, and *Pfu*) were combined with 0.5 mM each of dADP, dCDP, dGDP, and dTDP; 1 μM each of Primer4F and Primer4R; and 0.1 nM of 130-bp template in the buffer suggested by the manufacturer. The reaction proceeded at 95 °C for 30 s, 50 °C for 30 s, and 72 °C for 1 min for 16 cycles. Samples were analyzed on a 2% agarose gel and stained with ethidium bromide.

We considered the possibility that the DNA was replicated using small amounts of dNTPs present as contaminants in the dNDP samples. Analysis of the dNDP stocks by anion-exchange chromatography (Mono Q) revealed that the samples contained less than 1% species corresponding to dNTPs. For standard reactions that used 200 μM of each dNDP, at most 2 μM was in the triphosphorylated form; therefore, there would not be a sufficient amount of dNTPs to produce a full-length PCR product. In addition, if the polymerase exclusively utilized triphosphates, the substrates would be used up in early rounds of PCR, and the yield of the final product would not be comparable to the all-dNTP control reaction (Fig. 1*A*). The yields of our PCR reactions thus strongly suggested that dNDPs were utilized for DNA synthesis.

To rule out influence of any contaminating dNTPs or additives contaminating the dNDPs, buffers, and enzyme stocks, we purified the dNDPs using ion-exchange chromatography (see below), tested both commercial and house-purified enzymes, and prepared buffers from individual components, lacking betaine and detergents.

Short-primer extensions (Fig. 1 C and D). DNA polymerase assays were performed using purified dNDPs, noncommercial buffer (10 mM Tris·HCl, pH 7.4; 50 mM KCl, 5 mM $MgCl_2$), and either Template3A (Fig. 1*C*) or Template3C (Fig. 3*D*) at 50 nM, annealed with a 100-nM 5′ ^{32}P-labeled primer and incubated with about 1 U of enzymes. The reaction was preincubated at the extension temperature (60 °C for all enzymes other than *Bsu*, which was tested at 37 °C) and initiated by the addition of 100 μM of the final concentration of dNDPs, also preincubated at the reaction temperature. The reactions were stopped at various time points by removing aliquots of the polymerization reaction (2.5 μL) and adding them to a stop buffer (5 μL of 20 mM EDTA, 10 mM Tris·HCl, 8 M urea, and 0.1% SDS). Samples were heated to 95 °C for 5 min and fractionated on a denaturing 7.5% polyacrylamide gel. The gel was then exposed on a PhosphorImager screen (GE Healthcare) and analyzed using the Typhoon phosphorimager (GE Healthcare).

Long primer extensions (Fig. 1E and Fig. S2A). In vitro Taq DNA Polymerase extension assays were performed using a PAGE-purified 5′ ^{32}P-labeled Primer1bF with a calculated melting temperature of 72 °C and single-stranded Template1. The template was prepared using a modified asymmetric PCR protocol, where the reverse primer, Primer1bR, was in 20-fold excess of the biotinylated forward primer, Primer1bF. The forward primer was exhausted during the PCR cycling, resulting in ssDNA complementary to the 5′ ^{32}P-labeled primer. The biotinylated duplex was then removed using streptavidin magnetic beads, and the single-stranded template was ethanol-precipitated and resuspended for use in the kinetics experiments. The 10-nM 5′ ^{32}P-labeled primer, Primer1bF, was incubated with the single-stranded 6-nM DNA template, Template1, and 0.2 U Taq DNA polymerase in 1× standard Taq buffer at 95 °C for 1 min and then cooled to 72 °C. The polymerization reaction was initiated with the addition varying concentrations dADP (50 μM–1.5 mM) and a constant 200 μM of dTTP, dCTP, and dGTP. The reactions were stopped at various time points by removing aliquots of the polymerization reaction (2.5 μL) and adding them to a stop buffer (5 μL of 20 mM EDTA, 10 mM Tris·HCl, 8 M urea, and 0.1% SDS). Samples were heated to 95 °C for 5 min and fractionated on a denaturing 7.5% polyacrylamide gel. The gel was then exposed on a PhosphorImager screen (GE Healthcare) and analyzed using the Typhoon phosphorimager (GE Healthcare) and the GelAnalyzer software package. This experiment was repeated for dTDP.

Extension-time PCR assay. Two PCR reactions that included 1× Taq DNA buffer, 1 μM Primer1bF, 1 μM Primer1bR, 2.5 U Taq polymerase, 1 nM Template1, and 0.2 mM of either dNTP or dNDP were prepared. The reactions were divided into three separate tubes, and each was subjected to thermal cycling at 95 °C for 30 s and at 72 °C for 15 , 60 , or 120 s for 16 cycles. The reactions were then analyzed on a 2% agarose gel that contained ethidium bromide. The band intensities were analyzed using the GelAnalyzer software package.

qPCR of nucleotide diphosphate incorporation. The 0.5 μM each of Primer1bF and Primer1bR; 62 pM of Template1; 0.625 U of Taq DNA polymerase; 0.05–1 mM of dADP; 200 μM each of dTTP, dCTP, and dGTP; 20 nM of Oregon Green 488; and 0.3× SybrGreen in 1× standard Taq buffer were mixed on ice. The CFX96 Touch Real-Time PCR Detection System (BioRad) was used to perform and monitor the reaction for 45 cycles (95 °C for 30 s and annealing/extension at 72 °C for 1 min). Fluorescence data were analyzed using the CFX Manager Software (BioRad). Reactions were performed in triplicate and were repeated for the remaining three-nucleotide diphosphates.

Ion-exchange purification of dNDPs. Purification of dNDPs was carried out on an AKTA FPLC using a Mono Q 5/50 GL or DNAPac PA100 anion-exchange column. Nucleotides were loaded at a concentration of 5 mM (100 μL) in 10 mM Tris buffer, pH 7.4, and eluted off the column with a gradient of 10–500 mM of NH_4HCO_2 in 20-column volumes. On the Mono Q column, peak elutions varied among the nucleotides with dADP at 330 mM, dTDP at 287 mM, dCDP at 285 mM, and dGDP at 370 mM NH_4HCO_2. The nucleotides were dried and

resuspended in 20 μL of 10 mM Tris·HCl, pH 7.4. Elution of dNMPs or dNTPs occurred at significantly lower and higher salt concentrations, respectively, so that baseline resolution of the individual species was achieved.

Phosphate production assay. The 10 μM of Primer3 and Template3C was annealed in 1× ThermoPol buffer. Reaction with or without Taq polymerase and with either dNDPs or dNTPs was incubated at 72 °C for 3 min. The 1-μL aliquot of each reaction was mixed with 10 μL of 1 μM fluorescently labeled phosphate-binding protein (Life Technologies/Invitrogen) in 10 mM Tris·HCl, pH 7.5, and 20 mM NaCl and analyzed on a Falcon Optilux 384-well microplate with a fluorescence spectrophotometer (Biotek Synergy H1; excitation 420 nm, emission scanned from 450 to 600 nm). The $t = 0$ spectra (−Taq) were subtracted from the 3-min time points to detect phosphate production. Samples with dNDPs were treated separately from dNTPs, which showed some fluorescence buildup, but of equal magnitude in +Taq and −Taq experiments. Experiments with purified and unpurified dNDPs yielded similar phosphate buildup.

Single-nucleotide incorporation assay. A 40-nt gel-purified 5′ ^{32}P-labeled Primer3 (100 nM) was combined with a 100-nM purified unlabeled Template3G along with 1× ThermoPol buffer and 1.5 U Taq DNA polymerase. Reactions were heated to 95 °C for 1 min, cooled to room temperature, and incubated at a final temperature for the Arrhenius analysis. The reaction was started by the addition of purified dCDP, dADP, and dTDP at a 50-μM final concentration each (also preincubated at the final primer-extension temperature), and aliquots were quenched with equal volume of stop buffer (20 mM EDTA, 10 mM Tris·HCl, 8 M urea, and 0.1% SDS). Samples were fractionated on a denaturing 15% sequencing polyacrylamide gel and analyzed as described above, except that the bands were analyzed by drawing a line down each reaction lane in ImageJ; the line profile was exported to Igor Pro or Excel, and the bands were fit to a multi-Gaussian function. The number of Gaussians used corresponded to all bands observed and was kept constant for all experiments. The width of the Gaussians was also kept constant for all bands, based on the assumption that all bands diffuse equally during the course of the electrophoresis and phosphorimage exposure. The bands corresponding to the starting primer and the added dC, dA, and dT, followed by additional dA and dT, on template Template3G were easily distinguished, but required peak fitting for precise peak volume analysis, especially for weak peaks neighboring on strong peaks. We found that the Gaussian function modeled the peaks very well. For each nucleotide addition, the kinetics were calculated from initial rates of the fraction of the previous position extended.

Phosphorolysis assay. The 5-nM gel-purified 5′ ^{32}P-labeled primer, Primer3, was combined with a purified unlabeled 7.5-nM template, Template3G, in a 1:1.5 molar ratio, along with 1× standard Taq buffer (10 mM Tris·HCl, 50 mM KCl, and 1.5 mM $MgCl_2$ at pH 8.3) and 10 U Taq DNA polymerase. The sample was heated to 95 °C for 1 min and then cooled to 72 °C for 15 s at which point either 10 mM of potassium phosphate or potassium pyrophosphate was added to start the reaction. The reactions were incubated at 72 °C, and 2-μL aliquots were removed and added to stop buffer (2 μL, 20 mM EDTA, 10 mM Tris·HCl, 8 M urea, and 0.1% SDS) at time points of 1, 5, 10, and 20 min. Samples were fractionated and analyzed as described above.

TLC analysis of phosphorolysis products. Polyethyleneimine TLC plates (Sigma-Aldrich) were predeveloped with water to remove impurities and dried. The 100-nM Primer3–Template3T was incubated with 1× Taq buffer, 2.5 units of Taq polymerase, and ^{32}P-α–dATP. The internally labeled dsDNA was purified on nondenaturing PAGE. Reactions containing 100 nM dsDNA, 2.5 units of Taq polymerase, and 1× ThermoPol buffer supplemented with $MgCl_2$ to make 10 mM were prepared with no phosphate. Variable concentrations of sodium pyrophosphate or potassium phosphate (pH 7) were added at 72 °C to initiate the reverse reaction, and 0.5-μM aliquots were collected and spotted on the TLC plates, dried, and developed with 0.6 M LiCl and 2.5 mM Tris·HCl, pH 8.4. After the solvent front had reached the top of the plate, the plate was dried, exposed on a PhosphorImager screen (GE Healthcare), and analyzed using the Typhoon phosphorimager (GE Healthcare). The temperature study of the phosphorolysis reaction was performed with phosphate at 0.4 mM.

Arrhenius analysis. All kinetic data were plotted on $\ln(k_{obs})$ vs. $1/T(K)$ graphs derived from the Arrhenius equation $k = A^*\exp(-E_a/kT)$ linearized to $\ln(k) = \ln(A) - E_a/kT$, and the activation energy was extracted from the data by multiplying the slope of the linear portion of the graph (below 60 °C for the forward reaction) by the Boltzmann constant.

Model fitting. All data were fit with the stated models using the regression analysis in Excel. The activation energies were extracted directly from a line fit to the data with the reported errors being the SEs of the slope (multiplied by the Boltzmann constant).

Supporting Information contains DNA sequences and Figs. S1–S4.

ACKNOWLEDGMENTS. We thank T. Olsen, A. Halpern, J. Chaput, and G. Weiss for fruitful discussions and critical reading of the manuscript; the J. Chaput laboratory for a gift of homemade polymerases and use of their instruments; and A. Nikoomanzar for help with real-time detection of primer-extension reactions. This work was financially supported by the Pew Charitable Trusts (A.L. through the Pew Scholars in Biomedical Sciences Program) and by NIH Grant R01GM094929. This project/publication was made possible through the additional support of a grant from the John Templeton Foundation. The opinions expressed in this publication are those of the author(s) and do not necessarily reflect the views of the John Templeton Foundation.

1. Joyce CM, Steitz TA (1995) Polymerase structures and function: Variations on a theme? *J Bacteriol* 177:6321–6329.
2. Alberty RA, Goldberg RN (1992) Standard thermodynamic formation properties for the adenosine 5′-triphosphate series. *Biochemistry* 31:10610–10615.
3. Deutscher MP, Kornberg A (1969) Enzymatic synthesis of deoxyribonucleic acid. 28. The pyrophosphate exchange and pyrophosphorolysis reactions of deoxyribonucleic acid polymerase. *J Biol Chem* 244:3019–3028.
4. Perera L, et al. (2015) Requirement for transient metal ions revealed through computational analysis for DNA polymerase going in reverse. *Proc Natl Acad Sci USA* 112: E5228–E5236.
5. Kiefer JR, et al. (1997) Crystal structure of a thermostable Bacillus DNA polymerase I large fragment at 2.1 A resolution. *Structure* 5:95–108.
6. Kong H, Kucera RB, Jack WE (1993) Characterization of a DNA polymerase from the hyperthermophile archaea Thermococcus litoralis. Vent DNA polymerase, steady state kinetics, thermal stability, processivity, strand displacement, and exonuclease activities. *J Biol Chem* 268:1965–1975.
7. Hogrefe HH, Cline J, Lovejoy AE, Nielson KB (2001) DNA polymerases from hyperthermophiles. *Methods Enzymol* 334:91–116.
8. Brown HS, Licata VJ (2013) Enthalpic switch-points and temperature dependencies of DNA binding and nucleotide incorporation by Pol I DNA polymerases. *Biochim Biophys Acta* 1834:2133–2138.
9. Montgomery JL, Rejali N, Wittwer CT (2013) Stopped-flow DNA polymerase assay by continuous monitoring of dNTP incorporation by fluorescence. *Anal Biochem* 441:133–139.
10. Brune M, Hunter JL, Corrie JE, Webb MR (1994) Direct, real-time measurement of rapid inorganic phosphate release using a novel fluorescent probe and its application to actomyosin subfragment 1 ATPase. *Biochemistry* 33:8262–8271.
11. Freudenthal BD, Beard WA, Shock DD, Wilson SH (2013) Observing a DNA polymerase choose right from wrong. *Cell* 154:157–168.
12. Nakamura T, Zhao Y, Yamagata Y, Hua YJ, Yang W (2012) Watching DNA polymerase η make a phosphodiester bond. *Nature* 487:196–201.
13. Zahn KE, Tchesnokov EP, Götte M, Doublié S (2011) Phosphonoformic acid inhibits viral replication by trapping the closed form of the DNA polymerase. *J Biol Chem* 286: 25246–25255.
14. Rothwell PJ, et al. (2013) dNTP-dependent conformational transitions in the fingers subdomain of Klentaq1 DNA polymerase: Insights into the role of the "nucleotide-binding" state. *J Biol Chem* 288:13575–13591.
15. Towle-Weicksel JB, et al. (2014) Fluorescence resonance energy transfer studies of DNA polymerase β: The critical role of fingers domain movements and a novel non-covalent step during nucleotide selection. *J Biol Chem* 289:16541–16550.
16. Langer A, et al. (2015) Polymerase/DNA interactions and enzymatic activity: Multi-parameter analysis with electro-switchable biosurfaces. *Sci Rep* 5:12066.
17. Sluis-Cremer N, Arion D, Kaushik N, Lim H, Parniak MA (2000) Mutational analysis of Lys65 of HIV-1 reverse transcriptase. *Biochem J* 348:77–82.
18. Garforth SJ, Kim TW, Parniak MA, Kool ET, Prasad VR (2007) Site-directed mutagenesis in the fingers subdomain of HIV-1 reverse transcriptase reveals a specific role for the beta3-beta4 hairpin loop in dNTP selection. *J Mol Biol* 365:38–49.
19. Lewis DA, Bebenek K, Beard WA, Wilson SH, Kunkel TA (1999) Uniquely altered DNA replication fidelity conferred by an amino acid change in the nucleotide binding pocket of human immunodeficiency virus type 1 reverse transcriptase. *J Biol Chem* 274:32924–32930.
20. Yang G, Franklin M, Li J, Lin TC, Konigsberg W (2002) Correlation of the kinetics of finger domain mutants in RB69 DNA polymerase with its structure. *Biochemistry* 41:2526–2534.
21. Garforth SJ, Parniak MA, Prasad VR (2008) Utilization of a deoxynucleoside diphosphate substrate by HIV reverse transcriptase. *PLoS One* 3:e2074.
22. Gaucher EA, Govindarajan S, Ganesh OK (2008) Palaeotemperature trend for Precambrian life inferred from resurrected proteins. *Nature* 451:704–707.
23. Gaucher EA, Thomson JM, Burgan MF, Benner SA (2003) Inferring the palaeoenvironment of ancient bacteria on the basis of resurrected proteins. *Nature* 425:285–288.
24. Garcia AK, Schopf JW, Yokobori SI, Akanuma S, Yamagishi A (2017) Reconstructed ancestral enzymes suggest long-term cooling of Earth's photic zone since the Archean. *Proc Natl Acad Sci USA* 114:4619–4624.
25. Ronaghi M, Karamohamed S, Pettersson B, Uhlén M, Nyrén P (1996) Real-time DNA sequencing using detection of pyrophosphate release. *Anal Biochem* 242:84–89.
26. Rothberg JM, et al. (2011) An integrated semiconductor device enabling non-optical genome sequencing. *Nature* 475:348–352.
27. Nikoomanzar A, Dunn MR, Chaput JC (2017) Engineered polymerases with altered substrate specificity: Expression and purification. *Curr Protoc Nucleic Acid Chem* 69: 4.75.1–4.75.20.